

Probing Multi-Strange Dibaryon with Proton-Omega Correlation in High-energy Heavy Ion Collisions

Kenji Morita,^{1,*} Akira Ohnishi,^{1,†} Faisal Etminan,^{2,‡} and Tetsuo Hatsuda^{3,§}

¹*Yukawa Institute for Theoretical Physics, Kyoto University, Kyoto 606-8502, Japan*

²*Department of Physics, Faculty of Sciences, University of Birjand, Birjand 97175-615, Iran*

³*Theoretical Research Division, Nishina Center, RIKEN, Saitama 351-0198, Japan*

iTHES Research Group, RIKEN, Saitama 351-0198, Japan

(Dated: November 7, 2018)

The two-particle momentum correlation between the proton (p) and the Omega-baryon (Ω) in high-energy heavy ion collisions is studied to unravel the possible spin-2 $p\Omega$ dibaryon recently suggested by lattice QCD simulations. The ratio of correlation functions between small and large collision systems, $C_{SL}(Q)$, is proposed to be a new measure to extract the strong $p\Omega$ interaction without much contamination from the Coulomb attraction. Relevance of this quantity to the experimental observables in heavy-ion collisions is also discussed.

PACS numbers: 25.75.Gz, 21.30.Fe, 13.75.Ev

Introduction.— Baryon-baryon interactions serve as crucial inputs for understanding possible dibaryons with strangeness (S). In particular, the spin-0 H state with $S = -2$ [1] and the spin-2 nucleon-Omega ($N\Omega$) state with $S = -3$ [2] are among the most promising candidates for bound or resonant dibaryons, since the Pauli exclusion principle does not operate among quarks in these channels [3, 4]. Indeed, it was recently reported from first-principles lattice QCD simulations with heavy quark masses that there exist sizable attractions in the spin-0 H channel [5, 6] and in the spin-2 $N\Omega$ channel [7], although the quantitative answers would be obtained only by the on-going physical point simulations [8].

Experimentally, high-energy heavy ion collisions at the BNL Relativistic Heavy-Ion Collider (RHIC) and the CERN Large Hadron Collider (LHC) provide unique opportunities for multi-strange dibaryons [9]. For example, the search for the H -dibaryon has been conducted both at RHIC [10] and LHC [11]. More generally, the final state interactions for identical and non-identical hadrons after freeze-out [12, 13] have been shown to be sensitive to the low-energy scattering parameters [10, 14–19].

In this paper, motivated by the recent study on the $N\Omega$ interaction in lattice QCD [7], we study the proton-omega ($p\Omega$) correlation function in the relativistic heavy ion collisions to probe the nature of the $S = -3$ dibaryon. We propose that the ratio of the $p\Omega$ correlation functions with different source sizes is a good measure to extract the strong interaction between p and Ω without much contamination from the Coulomb attraction.

$N\Omega$ interaction.—In the S-wave $N\Omega$ system, there exist two possible channels, 5S_2 and 3S_1 , where ${}^{2s+1}L_J$ denotes the state with spin- s , L -wave, and total angu-

lar momentum J . As long as the strong interaction is concerned, the lowest threshold in octet-decuplet and decuplet-decuplet channels is $N\Omega$ at 2610 MeV. In the octet-octet channel, $\Lambda\Xi$ (with the threshold at 2430 MeV) and $\Sigma\Xi$ (at 2507 MeV) lie below $N\Omega$. For 5S_2 , the coupling of $N\Omega$ to these octet-octet channels occurs only through the D-wave, and thus it is dynamically suppressed. On the other hand, for 3S_1 , the sizable coupling to octet-octet channels through the rearrangement of quarks is expected in the S-wave.

Let us first consider the $N\Omega$ interaction in the 5S_2 channel where recent lattice QCD simulations with heavy quarks ($m_\pi=875$ MeV and $m_K=916$ MeV) show attraction for the entire range of their relative distance r [7]. In Fig. 1, the lattice data are shown by black circles with statistical error bars. The data can be fitted well by an attractive Gaussian core + an attractive (Yukawa)² tail with a form factor; $V(r) = b_1 e^{-b_2 r^2} + b_3 (1 - e^{-b_4 r^2})(e^{-b_5 r}/r)^2$, where $b_{1,3} < 0$ and $b_{2,4,5} > 0$. The best fit is shown by the red solid line in the figure denoted by V_{II} . Assuming that the qualitative form of this attractive potential does not change even for physical quark masses, we generate a series of potentials by varying the range-parameter at long distance, b_5 . Two typical examples are V_I with weaker attraction and V_{III} with stronger attraction in Fig. 1. By solving the Schrödinger equation using these potentials with the physical baryon masses, one finds no bound state for V_I , a shallow bound state for V_{II} , and a deep bound state for V_{III} . The binding energies, the scattering lengths¹ and the effective ranges in the 5S_2 $p\Omega$ channel with and without the Coulomb potential are summarized in Table I.

As for the $N\Omega$ interaction in the 3S_1 channel, there would be a strong coupling to the octet-octet channels

*Electronic address: kmorita@yukawa.kyoto-u.ac.jp

†Electronic address: ohnishi@yukawa.kyoto-u.ac.jp

‡Electronic address: fetminan@birjand.ac.ir

§Electronic address: thatsuda@riken.jp

¹ We use the “nuclear physics convention” in which the scattering phase shift δ at small momentum is given as $\delta = -ka_0$.

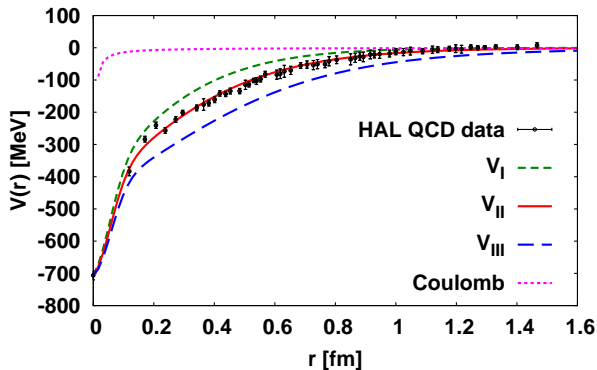


FIG. 1: Three typical examples of the $N\Omega$ potential. The black circles with error bars stand for the lattice QCD data with heavy quark masses [7]. The red line (V_{II}) corresponds to a fit to the lattice data with a Gaussian + (Yukawa)² form. The green short-dashed line (V_I) and the blue long-dashed line (V_{III}) denote the potentials with weaker and stronger attractions, respectively. The Coulomb potential for the $p\Omega$ system is also shown by the purple dashed line.

when the spatial distance between N and Ω becomes small. We model this by complete absorption of the $N\Omega$ wave function at short distance $r < r_0$. In other words, $V(r; {}^3S_1) = -iV_0\theta(r_0 - r)$ with $V_0 \rightarrow +\infty$ for the strong interaction part. We choose $r_0 = 2$ fm, because the Coulomb potential dominates over $V_{I,II,III}$ for $r > 2$ fm.

$N\Omega$ Correlation function.— The pairwise hadronic interaction gives enhancement or reduction of the observed number of pairs with small relative momenta in heavy ion collisions. In particular, the correlation function of non-identical pairs is directly related to the pairwise interaction due to the absence of the quantum statistical effect [13]. The $p\Omega$ correlation function is given in terms of the two-particle distribution $N_{p\Omega}(\mathbf{k}_p, \mathbf{k}_\Omega)$ normalized by the product of the single particle distributions, $N_\Omega(\mathbf{k}_\Omega)N_p(\mathbf{k}_p)$, with $\int_{x_i} \equiv \int d^4x_i$,

$$C(\mathbf{Q}, \mathbf{K}) = \frac{N_{p\Omega}(\mathbf{k}_p, \mathbf{k}_\Omega)}{N_p(\mathbf{k}_p)N_\Omega(\mathbf{k}_\Omega)} \quad (1)$$

$$\simeq \frac{\int_{x_p} \int_{x_\Omega} S_p(x_p, \mathbf{k}_p) S_\Omega(x_\Omega, \mathbf{k}_\Omega) |\Psi_{p\Omega}(\mathbf{r}')|^2}{\int_{x_p} S_p(x_p, \mathbf{k}_p) \int_{x_\Omega} S_\Omega(x_\Omega, \mathbf{k}_\Omega)},$$

where relative and total momenta are defined as $\mathbf{Q} = (m_p \mathbf{k}_\Omega - m_\Omega \mathbf{k}_p)/M$ and $\mathbf{K} = \mathbf{k}_p + \mathbf{k}_\Omega$, respectively, with $M \equiv m_p + m_\Omega$. The source functions $S_i(x_i, \mathbf{k}_i) \equiv E_i \frac{dN_i}{d^3\mathbf{k}_i d^4x_i}$, with $i = p, \Omega$ and $E_i = \sqrt{\mathbf{k}_i^2 + m_i^2}$, denote the phase space distribution of p and Ω at freeze-out. The final state interaction after the freeze-out is described by the two-particle wave function $\Psi_{p\Omega}$, in which the shift of the relative coordinate $\mathbf{r} = \mathbf{x}_\Omega - \mathbf{x}_p$ to $\mathbf{r}' = \mathbf{r} - \mathbf{K}(t_p - t_\Omega)/M$ accounts for the possible difference in the emission time between p and Ω . In the following, we assume that the pair purity is unity; i.e.

TABLE I: The binding energy (E_B), the scattering length (a_0) and the effective range (r_{eff}) with and without the Coulomb attraction in the $p\Omega$ system. Physical masses of the proton and Ω are used.

Spin-2 $p\Omega$ potentials		V_I	V_{II}	V_{III}
without Coulomb	E_B [MeV]	–	0.05	24.8
	a_0 [fm]	–1.0	23.1	1.60
	r_{eff} [fm]	1.15	0.95	0.65
with Coulomb	E_B [MeV]	–	6.3	26.9
	a_0 [fm]	–1.12	5.79	1.29
	r_{eff} [fm]	1.16	0.96	0.65

the weak decay contribution to p can be removed experimentally and that to Ω is negligible [10, 20].

Taking into account the spin degeneracy, we have $|\Psi_{p\Omega}|^2 = \frac{5}{8}|\Psi_5(\mathbf{r})|^2 + \frac{3}{8}|\Psi_3(\mathbf{r})|^2$, where Ψ_5 (Ψ_3) denotes the wave functions in spin-2 (spin-1) channel. The strong interaction is short ranged and modifies only the S-wave component of the wave function, so that we may write

$$\Psi_{5(3)}(\mathbf{r}) = [\psi^C(\mathbf{r}) - \psi_0^C(r)] + \chi_{\text{sc(abs)}}(r). \quad (2)$$

Here $\psi^C(\mathbf{r})$ is the Coulomb wave function characterized by the reduced mass $\mu = 601$ MeV and the Bohr radius $a_B = (\mu\alpha)^{-1} \simeq 45$ fm of the $p\Omega$ system. Its S-wave component is denoted by $\psi_0^C(r)$. The scattering wave function in the 5S_2 state, $\chi_{\text{sc}}(r)$, is obtained by solving the Schrödinger equation with both the strong interaction ($V_{I,II,III}$) and the Coulomb interaction.

Note that $\chi_{\text{sc}}(r)$ reduces to $\psi_0^C(r)$ in the absence of strong interaction. On the other hand, the wave function $\chi_{\text{abs}}(r)$ in the 3S_1 channel vanishes for $r \leq r_0$ due to our assumption of the complete absorption into octet-octet states², while it is identical to the Coulomb wave function for $r > r_0$:

$$\chi_{\text{abs}}(r) = \theta(r - r_0) \frac{1}{2i\bar{r}} (H_0^+(\bar{r}) - F(\bar{r}_0)H_0^-(\bar{r})). \quad (3)$$

Here $Q = |\mathbf{Q}|$, $\bar{r} = Qr$, $\bar{r}_0 = Qr_0$, and $H_{L=0}^+$ ($H_{L=0}^-$) is the outgoing (incoming) Coulomb function which reduces to $e^{+i\bar{r}}$ ($e^{-i\bar{r}}$) without the Coulomb force [21]. Note that $F(\bar{r}_0) = H_0^+(\bar{r}_0)/H_0^-(\bar{r}_0)$, so that $\chi_{\text{abs}}(r)$ is continuous across $r = r_0$. In the absence of the absorption, we have $\chi_{\text{abs}}(r)|_{r_0 \rightarrow 0} = \psi_0^C(r)$, since $F(\bar{r}_0 = 0) = 1$.

Case with static source.— We now consider the following static source function with spherical symmetry to

² For complete absorption ($V_0 \rightarrow +\infty$), the scattering length without the Coulomb interaction in the 3S_1 channel becomes $(\text{Re } a_0, \text{Im } a_0) = (r_0, 0)$, which is equivalent to the hard sphere with a radius r_0 . For finite V_0 , one has $\text{Re } a_0 < r_0$ and $\text{Im } a_0 < 0$ (see [18] for the analysis of baryon-antibaryon correlation function). We have checked that finite V_0 leads to a reduction of $C(Q)$ in the 3S_1 channel particularly for $Q < 50$ MeV, but the effect on the total $C(Q)$ is small, so that our conclusions are unchanged.

extract the essential part of physics;

$$S_i(x_i, \mathbf{k}_i) = \mathcal{N}_i E_i e^{-\frac{x_i^2}{2R_i^2}} \delta(t - t_i), \quad (i = p, \Omega). \quad (4)$$

Here R_i is a source size parameter, while \mathcal{N}_i is a normalization factor which cancels out between the numerator and denominator together with E_i in Eq.(1). Assuming the equal-time emission $t_p = t_\Omega$ for the moment, one obtains a concise formula,

$$\begin{aligned} C(Q) &= \int [dr] \int \frac{d\Omega}{4\pi} |\psi^C(\mathbf{r})|^2 \\ &+ \frac{5}{8} \int [dr] \{ |\chi_{sc}(r)|^2 - |\psi_0^C(r)|^2 \} \\ &+ \frac{3}{8} \int [dr] \{ |\chi_{abs}(r)|^2 - |\psi_0^C(r)|^2 \}, \quad (5) \end{aligned}$$

where $[dr] = \frac{1}{2\sqrt{\pi}R^3} dr r^2 e^{-\frac{r^2}{4R^2}}$ with $R = \sqrt{(R_p^2 + R_\Omega^2)}/2$ being the effective size parameter. $\int d\Omega$ is the integration over the solid angle between \mathbf{Q} and \mathbf{r} . Without the Coulomb interaction, the integration of the first line in Eq.(5) simply gives unity. The second (third) line is nothing but a spatial average of the difference between the S-wave probability density with and without the strong interaction, where the source function acts as a weight factor. A similar formula for the $\Lambda\Lambda$ correlation has been previously derived with the quantum statistical effect [16].

Let us now discuss, step by step on the basis of Eq.(5), the effects of the elastic scattering in the 5S_2 channel, the strong absorption in the 3S_1 channel and the long range Coulomb interaction. First, we neglect the Coulomb interaction, so that the first line of Eq. (5) is unity and $\psi_0^C(r)$ becomes the free spherical wave $j_0(\bar{r})$. For a weak attraction without bound state (V_I), the probability density $|\chi_{sc}(r)|^2$ in the 5S_2 channel is slightly enhanced from the free one at short distances and at small Q . This leads to $C(Q)$ represented by the green solid curve in Fig. 2(a) illustrated for a characteristic source size $R_p = R_\Omega = 2.5$ fm measured in the pp correlation for mid-central events [14, 15]. As the attraction increases towards and across the unitary limit where the scattering length diverges, the enhancement of $C(Q)$ becomes prominent as represented by the red solid curve corresponding to V_{II} in Fig. 2(a). As the attraction becomes even stronger, $\chi_{sc}(r)$ for small Q starts to oscillate and to be suppressed inside the source radius R due to large local momentum $q(r) = \sqrt{2\mu(E - V)}$. This effect tames the enhancement of $C(Q)$ and eventually leads to a suppression of $C(Q)$ as represented by the blue solid curve corresponding to V_{III} in Fig. 2(a).

In the 3S_1 channel, the probability density $|\chi_{abs}(r)|^2$ is zero at short distances. This implies that the absorption effect tends to suppress the particle correlation as indicated by the third line of Eq. (5). The dashed lines in Fig. 2(a) show $C(Q)$ with both the 5S_2 scattering and the 3S_1 absorption: The absorption effect is not negligibly small, but is not significantly large enough to change

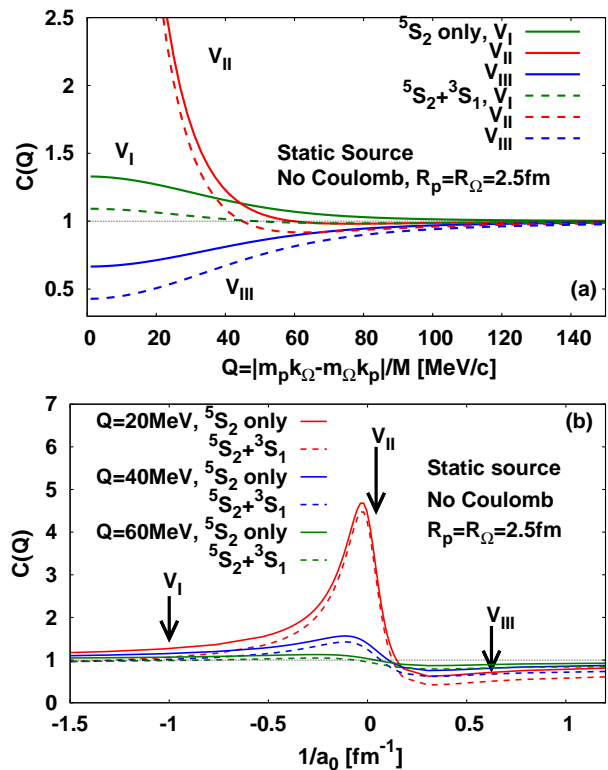


FIG. 2: $p\Omega$ correlation function for the static source with $R_p = R_\Omega = 2.5$ fm. The Coulomb interaction is switched off. (a) Solid (dashed) lines denote the correlations with only the 5S_2 scattering (with both the 5S_2 scattering and the 3S_1 absorption). (b) $C(Q)$ for $Q = 20, 40$ and 60 MeV as a function of a_0^{-1} obtained by changing the attraction of the $N\Omega$ potential through the parameter b_5 .

the qualitative behavior of $C(Q)$ obtained by the 5S_2 scattering alone.

Shown in Fig. 2(b) is $C(Q)$ without the Coulomb interaction for three typical momenta ($Q = 20, 40$, and 60 MeV) as a function of a_0^{-1} . By shifting the parameter b_5 in the $N\Omega$ potential, one can change the scattering length a_0 from negative to positive values without substantial change of the effective range r_{eff} : The arrows in the figure indicate a_0^{-1} corresponding to $V_{I,II,III}$. For weak (strong) attraction where $a_0^{-1} < 0$ ($a_0^{-1} > 0$), $C(Q)$ is enhanced (suppressed) from unity, while it is substantially enhanced around the unitary limit $a_0^{-1} = 0$. This implies that $C(Q)$ for a certain range of Q would provide a useful measure to identify the strength of the $N\Omega$ attraction.

Once we include the Coulomb interaction between the positively charged p and the negatively charged Ω , a strong enhancement of $C(Q)$ at small Q is introduced by the long-range attraction. The results with the Coulomb attraction are shown by the solid lines in Fig. 3(a) for $R_{p,\Omega} = 2.5$ fm. One finds that (i) the difference among three curves with $V_{I,II,III}$ in Fig. 2(a) is less visible in Fig. 3(a) at small Q due to the Coulomb enhancement,

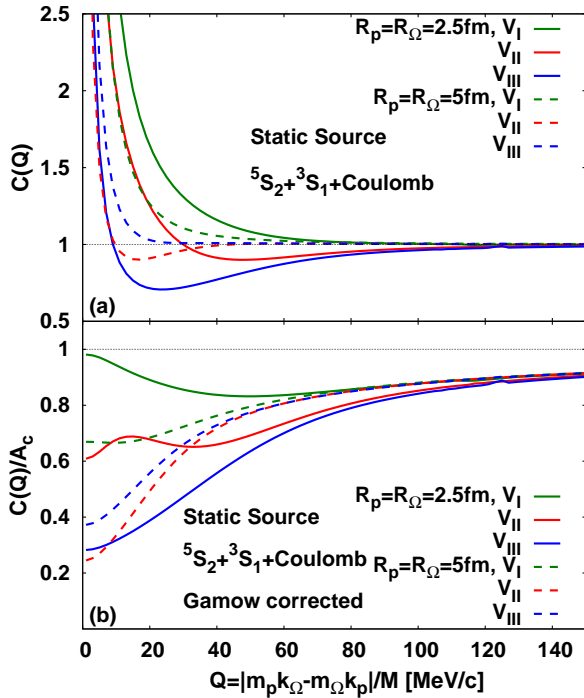


FIG. 3: (a) Correlation function with both strong and the Coulomb attractions for two different values of the static source sizes, $R_{p,\Omega} = 2.5$ fm (solid lines) and 5 fm (dashed lines). (b) Same correlation function as (a), but divided by the Gamow factor.

and (ii) the ordering of three curves become different especially due to the large reduction of the scattering length for V_{II} by the Coulomb effect (Table I). The dashed lines in Fig. 3(a) represent $C(Q)$ for larger source size, $R_{p,\Omega} = 5$ fm. In this case, the correlation function is more sensitive to the long-range part of the interaction as found for the proton-proton correlation [12, 13]. As a result, the ordering of the correlation function is further changed such that $C(Q)$ for V_{II} becomes the lowest.³

One may try to remove the Coulomb enhancement in Fig.3(a) by dividing $C(Q)$ by the $R_{p,\Omega}$ -independent Gamow factor, $A_c(\eta) = 2\pi\eta/(e^{2\pi\eta} - 1)$, with $\eta = -(Qa_B)^{-1}$ being the Sommerfeld parameter. Comparison of $C(Q)/A_c$ in Figure 3(b) and $C(Q)$ in Figure 2(a) indicates that the simple Gamow correction is not good enough to extract the characteristic feature of $C(Q)$ from the strong interaction: In principle, full Coulomb correction with source-size dependence is needed to isolate the effect of strong interaction. As an alternative and

³ For large R , the integrals in Eq. (5) are dominated by contributions from the outside of the potential range, where the wave functions are solely determined by the scattering phase shift. Then the effective range approximation for the S-wave scattering length leads to the Lednický-Lyuboshitz formula [12], in which $C(Q)$ is not sensitive to the potential shape [22] and is expressed in terms of low-energy scattering parameters.

model-independent way to handle the Coulomb effect, we propose to introduce an ‘‘SL (small-to-large) ratio’’ of the correlation functions for systems with different source sizes,

$$C_{\text{SL}}(Q) \equiv \frac{C_{R_{p,\Omega}=2.5\text{fm}}(Q)}{C_{R_{p,\Omega}=5\text{fm}}(Q)}, \quad (6)$$

as shown in Figure 4. An advantage of this ratio is that the effect of the Coulomb interaction for small Q is largely canceled, so that it has a good sensitivity to the strong interaction without much contamination from the Coulomb interaction.

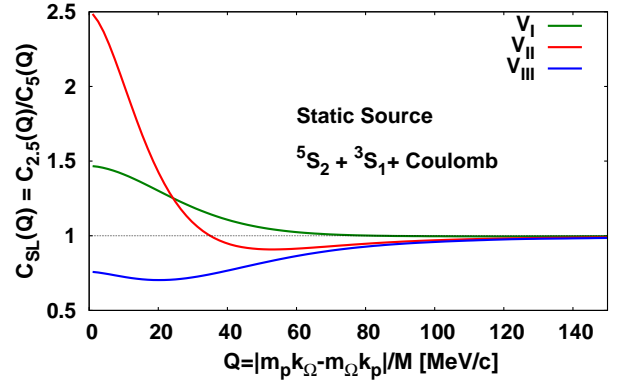


FIG. 4: $C_{\text{SL}}(Q)$ for the static source between the different source sizes, $R_{p,\Omega} = 2.5$ and 5 fm.

Effects of expansion and freeze-out time. — The results so far have been obtained with a simplified static source function (4). In reality, the collective expansion takes place in high energy heavy ion collisions. Also, the freeze-out of multi-strange hadrons may occur prior to other hadrons due to small cross sections [24, 25]. To see the influences of these dynamical properties, we consider the following source model with a 1-dim Bjorken expansion [23],

$$S(x_i, \mathbf{k}_i) = \mathcal{N}'_i E_i^{\text{tr}} \frac{1}{e^{E_i^{\text{tr}}/T_i} + 1} e^{-\frac{x^2 + y^2}{2(R_i^{\text{tr}})^2}} \delta(\tau - \tau_i), \quad (7)$$

where $E_i^{\text{tr}} = \sqrt{(\mathbf{k}_i^{\text{tr}})^2 + m_i^2} \cosh(y_i - \eta_s)$ with the momentum rapidity y_i and the space-time rapidity $\eta_s = \ln \sqrt{(t+z)/(t-z)}$. The temperature and the proper-time at the thermal freeze-out are denoted by T_i and τ_i , respectively. The transverse source size is denoted by the parameter R_i^{tr} . We have not taken into account the transverse collective expansion explicitly in the present paper, since its effect on $C(Q)$ has been shown to be effectively absorbed into a slight modification of R_i^{tr} as shown for the $\Lambda\Lambda$ correlation with the same model [16].

We consider a small system with $R_p^{\text{tr}} = R_\Omega^{\text{tr}} = 2.5$ fm and a large system with $R_p^{\text{tr}} = R_\Omega^{\text{tr}} = 5$ fm. Following the results of the dynamical analyses of the peripheral and central Pb+Pb collisions at $\sqrt{s_{NN}} = 2.76$ TeV with hydrodynamics + hadronic transport [24], we take

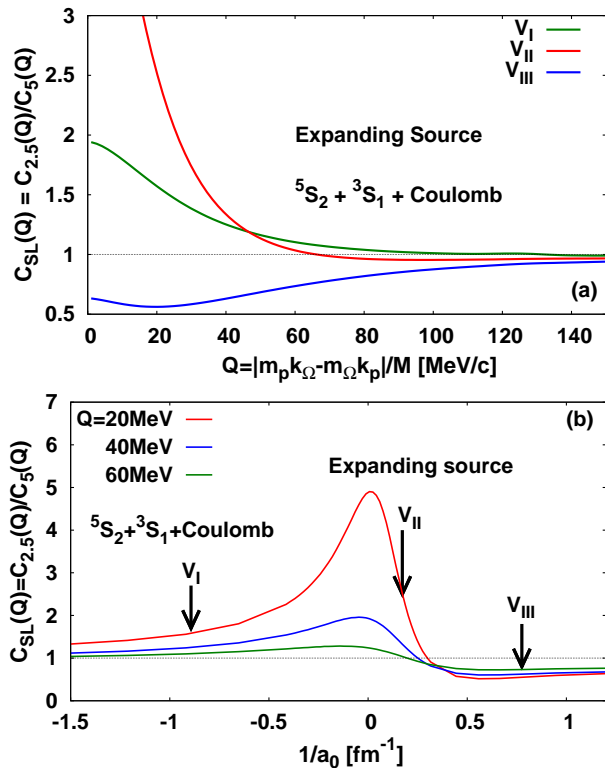


FIG. 5: (a) $C_{SL}(Q)$ as a function of (a) Q for three typical potentials (b) a_0^{-1} . In both figures, both the strong and Coulomb interactions are included.

τ_p (τ_Ω) = 3 (2) fm for the former, and τ_p (τ_Ω) = 20 (10) fm for the latter as characteristic values. We take $T_{p,\Omega} = 164$ MeV for peripheral collisions [26], while T_p (T_Ω) = 120 (164) MeV for central collisions [27]. Under the expanding source, Eq.(1) has explicit \mathbf{K} dependence: For illustrative purpose, we take the total longitudinal momentum to be zero $K_z = 0$ and the total transverse momentum to be $|\mathbf{K}^{tr}| = 2.0$ (2.5) GeV for peripheral (central) collisions which correspond to the twice the mean $|\mathbf{k}_p^{tr}|$ values of the proton [28].

Figure 5(a) demonstrates the effect of the dynamical property on $C_{SL}(Q)$: Its comparison to Fig.4 for the static source indicates no significant difference as far as the ratio $C_{SL}(Q)$ is concerned. Figure 5(b) shows $C_{SL}(Q)$ as a function of a_0^{-1} : Its comparison to Fig.2(b)

on $C(Q)$ implies that the strong $N\Omega$ interaction can be constrained by the measurements of this ratio. Moreover, taking the ratio of $C(Q)$ reduces the apparent reduction of its sensitivity to the strong interaction due to the purity factor. There are in principle two ways to extract $C_{SL}(Q)$ experimentally in ultrarelativistic heavy ion collisions at RHIC and LHC: (i) Comparison of the peripheral and central collisions for the same nuclear system, and (ii) comparison of the central collisions with different system sizes, e.g. central Cu+Cu collisions and central Au+Au collisions at RHIC.

Conclusion.— Motivated by the strong attraction at short distance between the proton and the Ω baryon in the spin-2 channel suggested by recent lattice QCD simulations, we studied the momentum correlation of $p\Omega$ emission from relativistic heavy ion collisions. Not only the elastic scattering in the spin-2 channel, but also the strong absorption in the spin-1 channel and the long-range Coulomb attraction are taken into account in our analysis. Depending on the strength of the $p\Omega$ attraction, the correlation function at small relative momentum changes substantially near the unitary limit. We have proposed that the ratio of the correlation function between the small and large collision systems, $C_{SL}(Q)$, is insensitive to the Coulomb interaction and to the source model of the emission. Thus it provides a useful measure to extract the strong interaction part of the $p\Omega$ attraction from the experiments at RHIC and LHC. Introduction of a realistic source model and relativistic treatment of $C(Q)$ [12] would be necessary for more quantitative evaluation at RHIC and LHC energies, which are left for further studies in the near future.

Acknowledgments

We thank HAL QCD Coll. for providing lattice data in Fig.1. This work was supported in part by the Grants-in-Aid for Scientific Research on Innovative Areas from MEXT (Nos. 24105008 and 24105001) and Grants-in-Aid for Scientific Research from JSPS (Nos. 15K05079, 15H03663, 16K05349, 16K05350). T.H. was supported in part by RIKEN iTHES Project. K.M. was supported in part by the National Science Center, Poland under grant: Maestro DEC-2013/10/A/ST2/00106.

[1] R. L. Jaffe, Phys. Rev. Lett. **38**, 195 (1977).
 [2] T. Goldman, K. Maltman, J. G. J. Stephenson, K. E. Schmidt, and F. Wang, Phys. Rev. Lett. **59**, 627 (1987).
 [3] M. Oka, Phys. Rev. D **38**, 298 (1988).
 [4] A. Gal, Acta Phys. Polon. B **47**, 471 (2016) [arXiv:1511.06605 [nucl-th]].
 [5] T. Inoue *et al.* [HAL QCD Collaboration], Prog. Theor. Phys. **124**, 591 (2010) [arXiv:1007.3559 [hep-lat]]; Phys. Rev. Lett. **106**, 162002 (2011) [arXiv:1012.5928 [hep-

lat]]; Nucl. Phys. A **881**, 28 (2012) [arXiv:1112.5926 [hep-lat]].
 [6] S. R. Beane *et al.* [NPLQCD Collaboration], Phys. Rev. Lett. **106**, 162001 (2011) [arXiv:1012.3812 [hep-lat]].
 [7] F. Etminan *et al.* [HAL QCD Collaboration], Nucl. Phys. A **928**, 89 (2014) [arXiv:1403.7284 [hep-lat]].
 [8] T. Doi *et al.* [HAL QCD Collaboration], arXiv:1512.01610 [hep-lat]; arXiv:1512.04199 [hep-lat].

- [9] S. Cho *et al.* [ExHIC Collaboration], Phys. Rev. Lett. **106**, 212001 (2011) [arXiv:1011.0852 [nucl-th]]; Phys. Rev. C **84**, 064910 (2011) [arXiv:1107.1302 [nucl-th]].
- [10] L. Adamczyk *et al.* [STAR Collaboration], Phys. Rev. Lett. **114**, 022301 (2015).
- [11] J. Adam *et al.* [ALICE Collaboration], Phys. Lett. B **752**, 267 (2016).
- [12] R. Lednicky and V. L. Lyuboshits, Sov. J. Nucl. Phys. **35**, 770 (1982), [Yad. Fiz. **35**, 1316 (1981)]; R. Lednicky, V. L. Lyuboshits, B. Erasmus and D. Nouais, Phys. Lett. B **373**, 30 (1996); R. Lednicky, Phys. Part. Nucl. **40**, 307 (2009).
- [13] See the reviews, W. Bauer, C. K. Gelbke and S. Pratt, Ann. Rev. Nucl. Part. Sci. **42**, 77 (1992). M. A. Lisa, S. Pratt, R. Soltz and U. Wiedemann, Ann. Rev. Nucl. Part. Sci. **55**, 357 (2005) [nucl-ex/0505014].
- [14] L. Adamczyk *et al.* [STAR Collaboration], Nature **527**, 345 (2015).
- [15] J. Adam *et al.* [ALICE Collaboration], Phys. Rev. C **92**, no. 5, 054908 (2015) [arXiv:1506.07884 [nucl-ex]].
- [16] K. Morita, T. Furumoto and A. Ohnishi, Phys. Rev. C **91**, no. 2, 024916 (2015) [arXiv:1408.6682 [nucl-th]].
- [17] A. Ohnishi, K. Morita, K. Miyahara and T. Hyodo, Nucl. Phys. **A954**, 294 (2016).
- [18] V. M. Shapoval, B. Erasmus, R. Lednicky and Y. M. Sinyukov, Phys. Rev. C **92**, no. 3, 034910 (2015).
- [19] B. O. Kerbikov, R. Lednicky, L. V. Malinina, P. Chaloupka and M. Sumbera, in *Proceedings, 44th Rencontres de Moriond on QCD and High Energy Interactions, : La Thuile, Italy, March 14-21, 2009*, edited by E. Augé, J. Dumarchez, B. Pietrzyk and J. Trân Thanh Vân, p. 403, [arXiv:0907.0617 [nucl-th]].
- [20] G. Agakishiev *et al.* [STAR Collaboration], Phys. Rev. Lett. **108**, 072301 (2012).
- [21] M. Abramowitz and I. A. Stegun, *Handbook of Mathematical Functions, With Formulas, Graphs, and Mathematical Tables*, (Dover, 1974).
- [22] M. Gmitro, J. Kvasil, R. Lednicky and V. L. Lyuboshits, Czech. J. Phys. B **36**, 1281 (1986).
- [23] S. Chapman, P. Scotto and U. W. Heinz, Heavy Ion Phys. **1**, 1 (1995) [hep-ph/9409349].
- [24] X. Zhu, F. Meng, H. Song, and Y. X. Liu, Phys. Rev. C **91**, 034904 (2015).
- [25] S. Takeuchi, K. Murase, T. Hirano, P. Huovinen, and Y. Nara, Phys. Rev. C **92**, 044907 (2015).
- [26] B. B. Abelev *et al.* [ALICE Collaboration], Phys. Lett. B **728**, 216 (2014) Erratum: [Phys. Lett. B **734**, 409 (2014)].
- [27] C. Shen, U. Heinz, P. Huovinen and H. Song, Phys. Rev. C **84**, 044903 (2011) [arXiv:1105.3226 [nucl-th]].
- [28] B. Abelev *et al.* [ALICE Collaboration], Phys. Rev. C **88**, 044910 (2013) [arXiv:1303.0737 [hep-ex]].